5 (2026) 100292

Contents lists available at ScienceDirect

Journal of Subatomic Particles and Cosmology

journal homepage: https://www.sciencedirect.com/journal/journal-of-subatomic-particles-and-cosmology

Full Length Article

Probing J/ψ, η_c and h_c resonances in proton-lead collisions at the LHC

Sudhansu S. Biswal [a], Sushree S. Mishra [a,*], Monalisa Mohanty [a], K. Sridhar [b]

[a] Department of Physics, Ravenshaw University, Cuttack, 753003, India
[b] School of Arts and Sciences, Azim Premji University, Sarjapura, Bangalore, 562125, India

ARTICLE INFO

Keywords:
Charmonia
NRQCD
Modified NRQCD
Heavy-ion collision

ABSTRACT

After achieving a successful description of charmonia production in pp collisions within Non-Relativistic Quantum Chromodynamics (NRQCD) and modified NRQCD (MNRQCD) frameworks, we now extend our study to pPb collisions at the Large Hadron Collider (LHC). In this context, theoretical predictions for the production cross-section, the nuclear modification factor R_{pPb} and forward - to - backward production ratio R_{FB} of J/ψ have been made as a function of transverse momentum and rapidity at the LHC. MNRQCD provides a reasonable agreement with the available LHC data for J/ψ production. Furthermore, using the heavy quark symmetry relation, we have estimated the production cross sections and expected number of events of η_c and h_c production in both NRQCD and MNRQCD. Notably, the predictions exhibit substantial differences in the integrated cross-sections as well as in the p_T distributions for these states at the LHC, highlighting the importance of further experimental and theoretical studies of these resonances to advance our understanding of quarkonium production.

Three decades ago, it was proposed that the formation of Quark - Gluon Plasma (QGP) [1–3] would reduce the yield of J/ψ mesons in high-energy heavy ion collisions compared to proton-proton (pp) collisions. This suppression was attributed to the Debye screening of the heavy-quark potential at finite temperatures. This predicted signature of QGP shows significant experimental and theoretical research into the production of heavy quarkonium in nuclear collisions. The Relativistic Heavy Ion Collider (RHIC) [4,5] and the Large Hadron Collider (LHC) [6–9] are the best experimental facilities that are designed to investigate an exotic state of matter such as the QGP which has been studied both at the perturbative and non-perturbative sector of QCD. The investigation of heavy quarkonium bound states in heavy-ion collisions [10,11] play a crucial role in exploring the properties of the deconfined QCD matter. This study examines proton-lead (pPb) collisions, where the behavior of heavy quarkonium bound states offer valuable insights into the formation and properties of the QGP.

In contrast to pp collisions, quarkonium production in pPb collisions is affected by cold nuclear matter effects, primarily arising from modifications of the parton distributions inside the nucleus. These lead to deviations in the production cross-sections, quantified with the nuclear modification factor R_{pPb} and result in a forward - to - backward ratio deviates from unity, making pPb collisions a crucial probe to distinguish nuclear effects from the pp production.

In relativistic heavy-ion collisions, charm quark pairs are generated during the early stages of the interaction, but their conversion into charmonium bound states occur more gradually. This distinction underscores the complex dynamics of particle production and hadronization in heavy-ion collisions. In particular, J/ψ meson production serves as a crucial observable for studying the QGP [12] – a high-temperature, deconfined state of matter where quarks and gluons exist freely, rather than being confined within hadrons. Some of the theoretical predictions in heavy ion collisions [13–18] have also been tested emphasizing the statistical hadronization at the LHC energies, which indicate that the production mechanisms can significantly enhance charmonium yields, highlighting the need to incorporate long-distance dynamics when extending MNRQCD model to heavy-ion collisions. To improve our understanding of the QGP, some analysis in pp and pA collisions are necessary.

Charmonia serve as particularly powerful probes for studying the QGP. The production of charmonia can indeed be effectively studied using Non-Relativistic Quantum Chromodynamics (NRQCD) [19], which is a powerful theoretical framework that simplifies the calculations of heavy quarkonium production and dynamics by exploiting the non-relativistic nature of the heavy quarks and anti-quarks when their relative velocity is small compared to the speed of light.

In NRQCD at leading order, the $Q\bar{Q}$ state is in a color-singlet state, however at $O(v)$, which defines at the order of the relative velocity of

* Corresponding author.
E-mail addresses: ssbiswal@ravenshawuniversity.ac.in (S.S. Biswal), sushreesimran.mishra97@gmail.com (S.S. Mishra), monalimohanty97@gmail.com (M. Mohanty), sridhar.k@apu.edu.in (K. Sridhar).

https://doi.org/10.1016/j.jspc.2026.100292
Received 11 November 2025; Received in revised form 16 January 2026; Accepted 19 January 2026
Available online 22 January 2026

quark-antiquark pair, can be in a color-octet state which is connected to the physical quarkonium state through a non-perturbative gluon emission. The cross-section for the production of a quarkonium state H of mass M in NRQCD can be expressed as:

$$\sigma(H) = \sum_{n=\{\alpha,S,L,J\}} \frac{F_n}{M^{d_n-4}} \langle \mathcal{O}_n^H(^{2S+1}L_J)\rangle, \tag{1}$$

where F_n's are the short-distance coefficients and $\mathcal{O}_n$ are operators of naive dimension d_n, describing the long-distance effects. Due to NRQCD factorization, the non-perturbative matrix elements are energy independent and can be extracted at a given energy and used in the prediction of quarkonium cross-sections at other energies.

NRQCD has been more successful in explaining the systematics of quarkonium production at the Fermilab Tevatron [20,21], compared to the then existing Color Singlet Model (CSM) [22], which was used to analyze the production of quarkonia, where the $Q\bar{Q}$ state produced in the short-distance process was assumed to be a color-singlet. NRQCD predicts transverse polarisation for quarkonia production at high p_T, but experiments fail to see any evidence for the polarisation in J/ψ [23] or Υ [21,24,25] measurements. Therefore, independent tests of NRQCD [26–31] are important and the prediction of polarisation of the produced quarkonium state is an important test to study the discrepancy between the predictions made by NRQCD for the quarkonium polarisation at high p_T, thereby addressing a longstanding puzzle in high-energy collisions.

In Refs. [32–35], we have studied quarkonia production, where we get a significant difference between the NRQCD and modified NRQCD (MNRQCD) model in case of η_c, η_b, h_c and h_b production. However, MNRQCD predictions for η_c and h_c production shows good agreement with LHCb experimental results. Motivated by the success of MNRQCD in the pp collisions, we have extended our work to study charmonia production in heavy ion collisions. In this paper, we have focused our analysis on charmonia production in pPb collisions using both NRQCD and MNRQCD models.

The NRQCD formula for J/ψ can be written explicitly in terms of the various octet and singlet intermediate states:

$$\sigma_{J/\psi} = \hat{F}_{^3S_1^{[1]}} \times \langle \mathcal{O}(^3S_1^{[1]})\rangle + \hat{F}_{^3S_1^{[8]}} \times \langle \mathcal{O}(^3S_1^{[8]})\rangle + \hat{F}_{^1S_0^{[8]}} \times \langle \mathcal{O}(^1S_0^{[8]})\rangle + \frac{1}{M^2}\left[\hat{F}_{^3P_J^{[8]}} \times \langle \mathcal{O}(^3P_J^{[8]})\rangle\right]. \tag{2}$$

The above formula gets modified to the following in the MNRQCD with perturbative soft gluon emission:

$$\begin{aligned}\sigma_{J/\psi} \;=\; & \left[\hat{F}_{^3S_1^{[1]}} \times \langle \mathcal{O}(^3S_1^{[1]})\rangle\right] \\ & + \left[\hat{F}_{^3S_1^{[8]}} + \hat{F}_{^1P_1^{[8]}} + \hat{F}_{^1S_0^{[8]}} + (\hat{F}_{^3P_J^{[8]}})\right] \times \left(\frac{\langle \mathcal{O}(^3S_1^{[1]})\rangle}{8}\right) \\ & + \left[\hat{F}_{^3S_1^{[8]}} + \hat{F}_{^1P_1^{[8]}} + \hat{F}_{^1S_0^{[8]}} + (\hat{F}_{^3P_J^{[8]}})\right] \times \langle \mathcal{O}\rangle,\end{aligned} \tag{3}$$

where

$$\langle \mathcal{O}\rangle = \times\left[\langle \mathcal{O}(^3S_1^{[8]})\rangle + \langle \mathcal{O}(^1S_0^{[8]})\rangle + \frac{\langle \mathcal{O}(^3P_J^{[8]})\rangle}{M^2}\right]. \tag{4}$$

The differential cross section for $c\bar{c}$ pair production with specific angular momentum and color states at the LHC is given by:

$$\begin{aligned}&\frac{d\sigma}{dp_T}\,(p\;Pb \to c\bar{c}\;[^{2S+1}L_J^{[1,8]}]\,X) = \\ &\sum \int dy \int dx_1\; x_1 G_{a/p}(x_1)\; x_2 G_{b/Pb}(x_2) \frac{4p_T}{2x_1 - \bar{x}_T e^y} \\ &\frac{d\hat{\sigma}}{d\hat{t}}(ab \to c\bar{c}[^{2S+1}L_J^{[1,8]}]\;d),\end{aligned} \tag{5}$$

where the summation is over the partons (a and b), the final state $c\bar{c}$ is in the $^1S_0^{[8]}$, $^1P_1^{[8]}$, $^3S_1^{[8]}$ states and $G_{a/p}$, $G_{b/Pb}$ are the distributions of partons a and b in the proton and lead respectively. Here, x_1 and x_2 are the respective momentum they carry. In the above formula, $\bar{x}_T = \sqrt{x_T^2 + 4\tau} \equiv 2M_T/\sqrt{s}$ with $x_T = 2p_T/\sqrt{s}$ and $\tau = M^2/s$. $\sqrt{s}$ is the center-of-mass energy, M is the mass of the resonance and y is the rapidity at which the resonance is produced. The non-perturbative parameters used in our analysis are taken from Ref. [36] and the charm-quark mass is 1.2730 GeV [37]. Here nuclear Parton Distribution Functions [38] for the nucleus are as follows:

$$G_{b/Pb}(x_2) = \frac{Z}{A}G^{p/A}(x_2) + \frac{A-Z}{A}G^{n/A}(x_2). \tag{6}$$

The fixed-order perturbative calculation have been used to get the cross-section for charmonia production and a cut-off is imposed in the calculations for low-p_T regime. The charmonia cross-section in the low-p_T region requires a resummation of multiple gluon radiation.

Fig. 1 shows the fit to the 200 GeV RHIC data [39] correspond to pp collisions on J/ψ production, where $B_{||}$ is the branching ratio for $J/\psi \to e^+e^-$ (5.973%), including branching ratio for $J/\psi \to \gamma e^+e^-$ (0.88%) [37].

Using a linear fit, we extract the fitted parameter for J/ψ production to be -0.153 GeV^3. The fit yields $\chi^2/NDF < 1$ with the confidence level more than 99% and the uncertainty in the fitted parameter is <0.1%, which demonstrate the robustness of the fit and the high statistical significance of the result.

Our analysis tests the energy independence of the extracted non-perturbative parameter. Unless given by some factorisation theorem, this independence cannot be assumed a priori. The agreement with LHC data demonstrates that the non-perturbative parameter remains energy independent, as theoretically expected.

In Fig. 2, the theoretical production cross-sections for J/ψ have been compared with the LHC [6–9] experimental data for prompt production, showing an agreement with MNRQCD for pPb collisions. Here while comparing with the CMS and ATLAS experimental results, we have taken the branching ratio for $J/\psi \to \mu^+\mu^-$ (5.961%) for theoretical predictions of J/ψ production.

We have made our analysis using different sets of LDMEs, nCTEQ15 nuclear PDFs and scale to vary from $Q = \frac{M_T}{2}$ to $Q = 2M_T$, taking $Q = M_T$ as the central scale to determine the cross-section for the J/ψ production. The resulting predictions are found to be reasonable with the measured data within the given kinematic range. To this end, we have shown the theoretical uncertainty band with results to the variation of scale in Fig. 3, comparing our MNRQCD prediction with the LHCb experiment. Similar observations are obtained for other LHC measurements.

Nuclear modification factor is defined as the ratio of the yield in heavy-ion collisions to that in pp collisions, scaled by the average number of binary collisions. Here the nuclear modification factor for pPb configuration is:

$$R_{pPb}(p_T,|y|) = \frac{1}{208}\frac{d^2\sigma_{pPb}/dp_T dy}{d^2\sigma_{pp}/dp_T dy}, \tag{7}$$

where, σ_{pp} is the cross-section from pp collisions.

The formula for forward-to-backward ratio is defined as:

$$R_{FB}(p_T,|y|) = \frac{d^2\sigma_{pPb}(p_T,+|y|)/dp_T dy}{d^2\sigma_{pPb}(p_T,-|y|)/dp_T dy}. \tag{8}$$

Figs. 4 and 5 show the nuclear modification factor and forward-to-backward production ratio predictions using MNRQCD model, which gives significant results while comparing with the experimental data. Here, the MNRQCD model successfully reproduces the kinematic dependence of both the nuclear modification factor ($R_{\rm pPb}$) and the forward-to-backward ratio ($R_{\rm FB}$) across the transverse momentum and rapidity ranges, while comparing with the experimental data. The Figs. 4 and 5 suggest that $R_{\rm pPb}$ and $R_{\rm FB}$ work as a good observable up to at least $p_T \sim$ 14 GeV, exhibiting a stable behavior around unity.

In Figs. 4 and 5, the LHC data, we have taken in the different rapidity ranges have relatively larger statistical and systematic uncertainties. Hence, the theoretical predictions based on these bin-averaged values

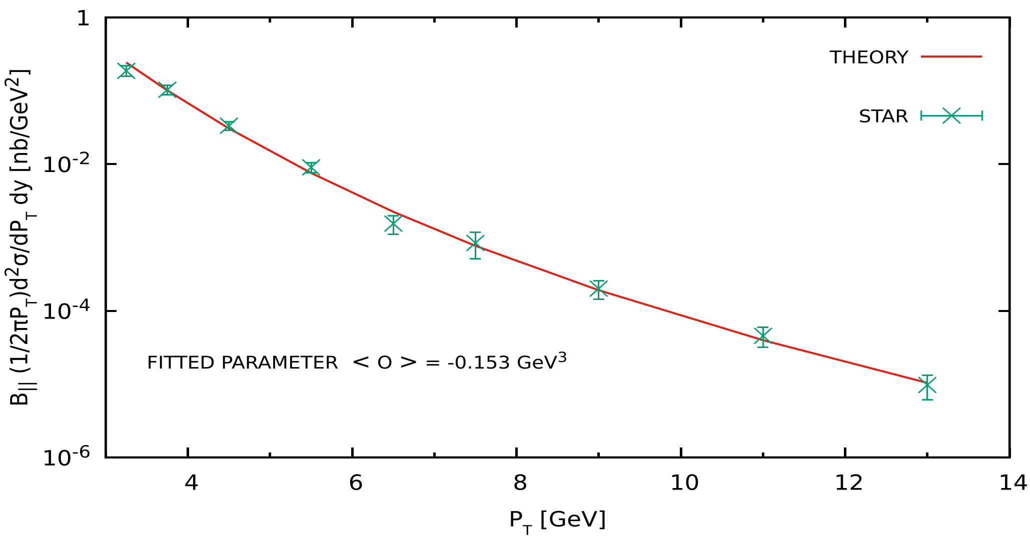

Fig. 1. Theoretical prediction of differential cross sections fitted to the data on J/ψ production in pp collisions from the STAR experiment at RHIC.

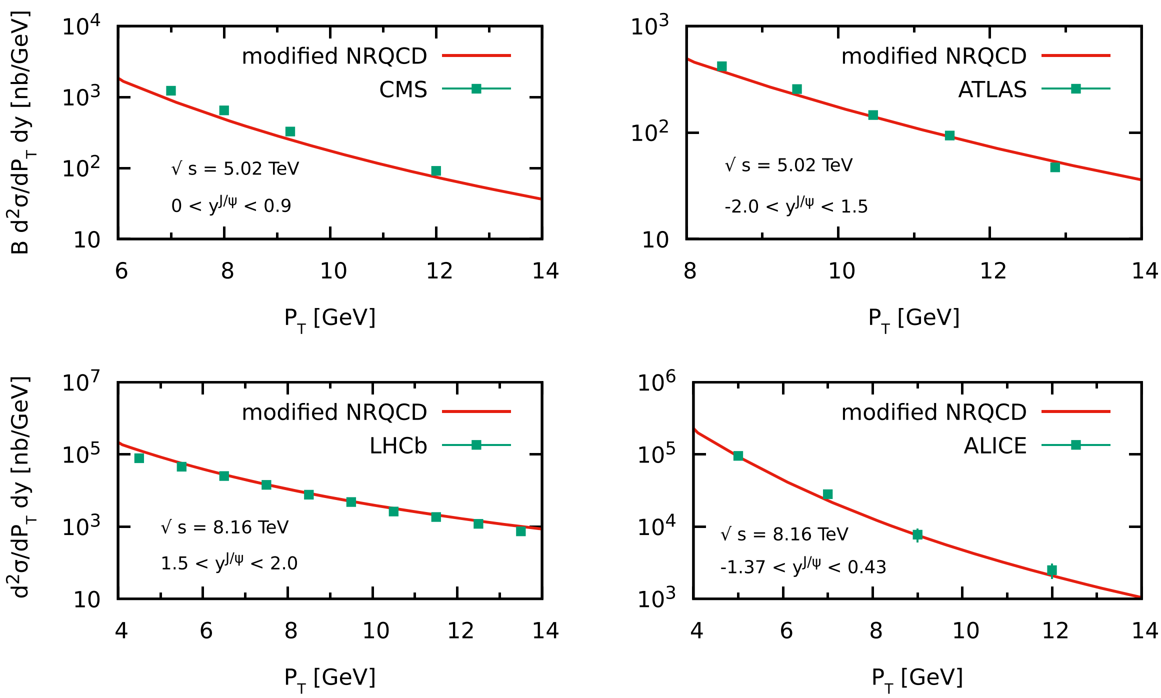

Fig. 2. Predicted differential distributions for J/ψ in pPb collisions production compared to the data from the LHC experiments.

Table 1
Number of η_c events expected at the LHC correspond to integrated luminosity of 100 nb^{-1}.

	~Expected number of events			
	Rapidity: $\lvert y\rvert < 1.5$, $\sqrt{s}$ = 5.02 TeV		Rapidity: $2 < y < 4$, $\sqrt{s}$ = 8.16 TeV	
Model	P_T > 5 GeV	P_T > 10 GeV	P_T > 5 GeV	P_T > 10 GeV
NRQCD	1.8×10^5	2.3×10^4	1.2×10^5	1.5×10^4
MNRQCD	5.5×10^4	4.2×10^3	3.4×10^4	2.6×10^3

Table 2
Number of h_c events expected at the LHC correspond to integrated luminosity of 100 nb^{-1}.

	~Expected number of events			
	Rapidity: $\lvert y\rvert < 1.5$, $\sqrt{s}$ = 5.02 TeV		Rapidity: $2 < y < 4$, $\sqrt{s}$ = 8.16 TeV	
Model	P_T > 5 GeV	P_T > 10 GeV	P_T > 5 GeV	P_T > 10 GeV
NRQCD	9.3×10^2	45	5.5×10^2	25
MNRQCD	3.0×10^4	3.0×10^3	1.9×10^4	1.8×10^3

may not fully reproduce the detailed shape of the experimental distributions.

For better understanding, we have extended our work on p_T distributions of η_c and h_c production in both NRQCD and MNRQCD. Figs. 6 and 7 represent the η_c production differential cross-sections as a function of p_T and integrated cross-sections for different p_T - cuts in both NRQCD and MNRQCD. Similarly, Figs. 8 and 9 are for h_c production. We study η_c in its decay into $p\bar{p}$ with a branching fraction of 1.33×10^{-3} [37]. For h_c production in its decay into η_c and γ with a branching fraction of 60% and η_c in its decay into $p\bar{p}$ with a branching fraction of 1.33×10^{-3}. As can be seen, both NRQCD and MNRQCD show significant deviations from their respective predictions for η_c as well as h_c production.

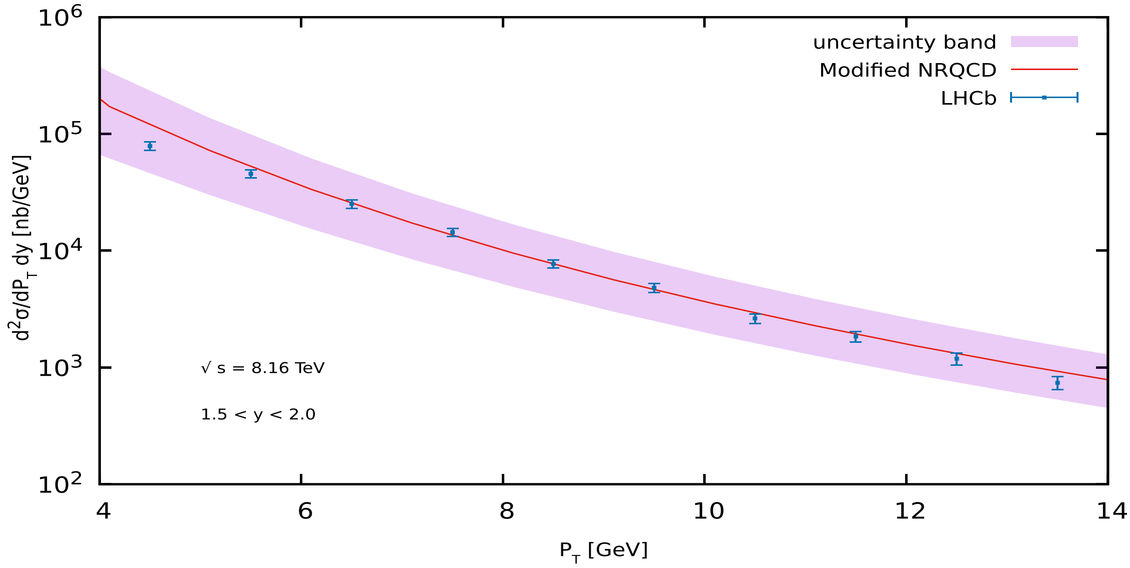

Fig. 3. Predicted differential distributions for J/ψ in pPb collisions production compared to the data from the LHCb experiment. The band represents the variation in the p_T distribution cross-section by changing the scale from $\frac{M_T}{2}$ to $2M_T$.

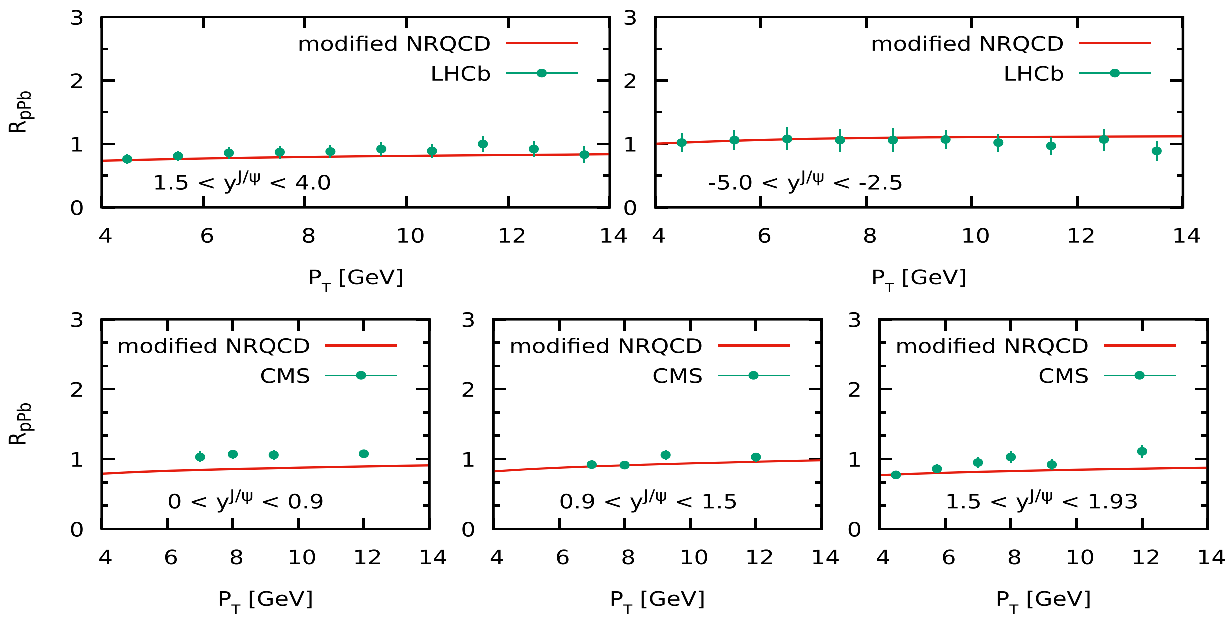

Fig. 4. Transverse momentum dependence of $R_{\rm pPb}$ for J/ψ production in pPb collisions at the LHC.

The novel feature about MNRQCD is the mixed octet-singlet contribution. The single extracted parameter is a result of a balance between the singlet, the octet-singlet and the pure octet term. In η_c and h_c production, the MNRQCD cross-section is smaller than that in NRQCD due to the fitted non-perturbative parameter extracted from J/ψ and χ_c respectively. Now which of these agree with the data is a question that only experiments can settle and therein lies the new and interesting contribution of this present paper. The pPb collisions are incorporated through the use of nuclear Parton Distribution Functions (nPDFs) for the lead nucleus and proton PDFs, introducing transverse momentum and rapidity dependent nuclear modifications, that are absent in pp collisions. However, the MNRQCD framework offers resolution of the LHCb η_c anomaly, successfully explaining the observed discrepancies, demonstrating a good agreement with the LHCb experimental results for different center of mass energies.

To get a sense of the feasibility of measuring the η_c and h_c production at the LHC, we have calculated the p_T -integrated cross sections in two different rapidity ranges. These results, presented in Tables 1 and 2 for an integrated luminosity of 100 nb^{-1}, suggest that a significant number of η_c and h_c events can be expected at the LHC.

In conclusion, we have studied J/ψ production in MNRQCD for pPb collisions. We have fitted our model predictions to STAR data on J/ψ production and used the fitted parameters to predict the distributions at the LHC energy, and find an agreement with the data from the CMS, LHCb, ALICE and ATLAS experiment. The nuclear modification factors and forward-to-backward ratios for J/ψ show an agreement, when compared with the data from the LHC experiment. Furthermore, we have made predictions for η_c and h_c production using both NRQCD and MNRQCD, which give an insight to the charmonia production in heavy ion collisions. In future, if the measurements of η_c and h_c become

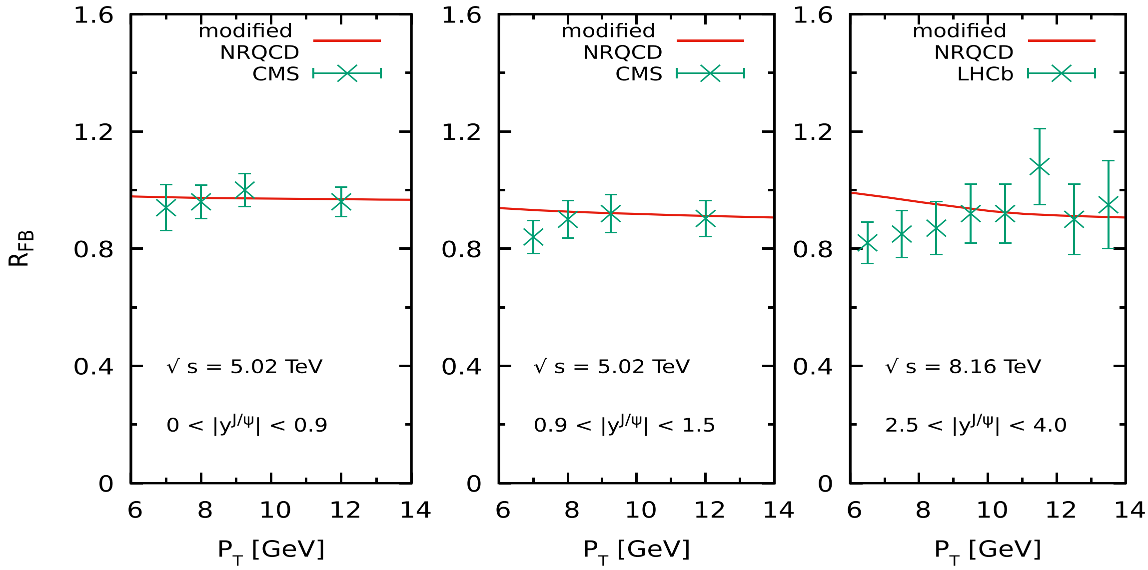

Fig. 5. Transverse momentum dependence of R_{FB} for J/ψ production in pPb collisions at the LHC.

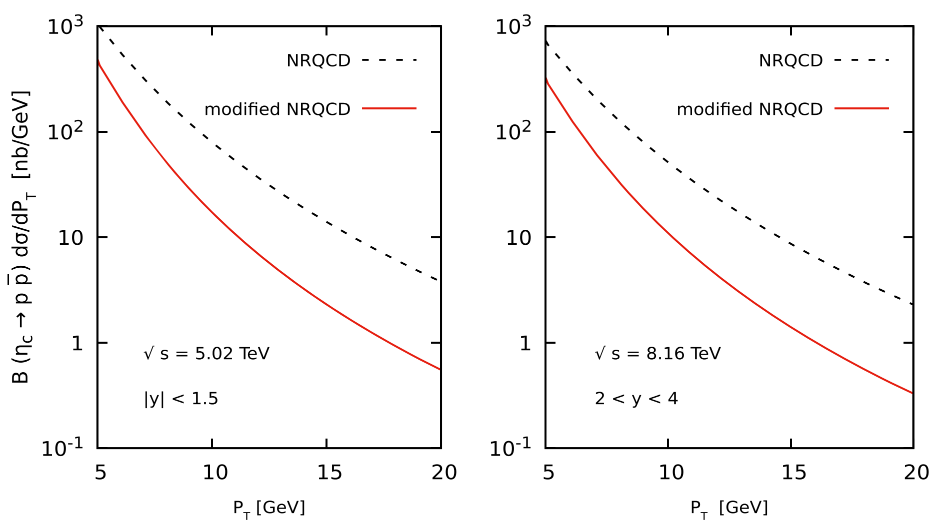

Fig. 6. Predicted differential cross-sections for η_c production in pPb collisions at the LHC.

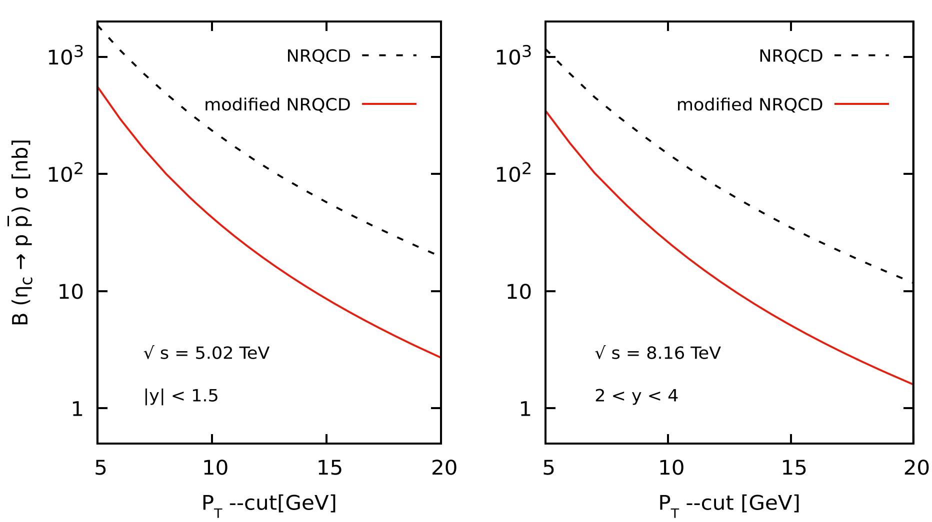

Fig. 7. Predicted Integrated cross-sections for η_c production in pPb collisions at the LHC.

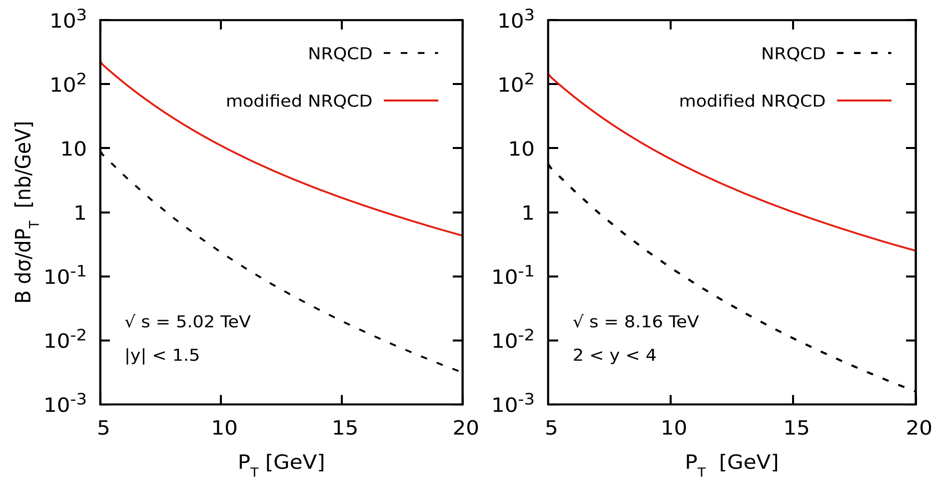

Fig. 8. Predicted differential cross-sections for h_c production in pPb collisions at the LHC.

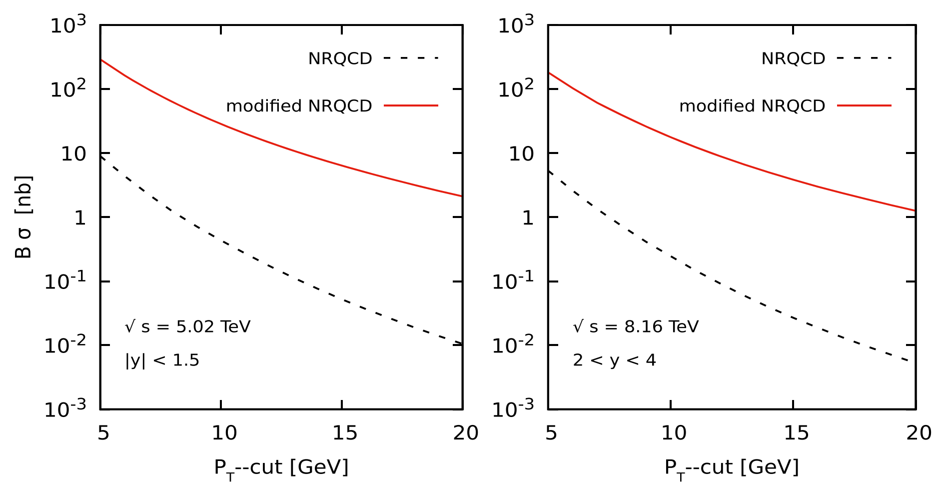

Fig. 9. Predicted Integrated cross-sections for h_c production in pPb collisions at the LHC.

available, they will be experimentally challenging due to the difficulty in reconstructing its decay channels, which effectively leads to a suppressed production cross section. However, with upcoming detector upgrades at the LHC and the HL-LHC, such measurements may become feasible, offering a valuable opportunity to discriminate between NRQCD and MNRQCD predictions and thereby deepen our understanding of heavy-quarkonium production. In particular, beyond the improved agreement of MNRQCD with the data compared to NRQCD, our study demonstrates the energy independence of the extracted non-perturbative parameter across the RHIC and the LHC energies, providing a nontrivial consistency check of the underlying factorization assumptions. Furthermore, the successful description of different experimental datasets imposes quantitative constraints on the universality of the non-perturbative input, thereby offering new insight into quarkonium production dynamics within the MNRQCD framework.

CRediT authorship contribution statement

Sudhansu S. Biswal: Writing – review & editing, Visualization, Validation, Supervision, Methodology, Investigation, Formal analysis, Conceptualization; **Sushree S. Mishra:** Writing – original draft, Visualization, Validation, Methodology, Investigation, Formal analysis, Conceptualization; **Monalisa Mohanty:** Writing – review & editing, Visualization, Validation, Methodology, Investigation, Formal analysis, Conceptualization; **K. Sridhar:** Writing – review & editing, Visualization, Validation, Supervision, Methodology, Investigation, Formal analysis, Conceptualization.

Data availability

No data was used for the research described in the article.

Declaration of competing interest

The authors declare that they have no known competing financial interests or personal relationships that could have appeared to influence the work reported in this paper.

Acknowledgments

One of us (K.S.) gratefully acknowledges a research grant (No. 122500) from the Azim Premji University. In this paper, as in everything else he writes, the results, opinions and views expressed are K.S.'s own and are not that of the Azim Premji University.

References

[1] T. Matsui, H. Satz, Phys. Lett. B 178 (1986) 416–422.
[2] R. Pasechnik, M. Šumbera, 3, (2017), 1–7. Hep-ph, arxiv:1611.01533.
[3] J.P. Blaizot, D.D. Boni, P. Faccioli, G. Garberoglio, Nucl. Phys. A 946 (2016) 49–88. Nucl-th, arXiv:1503.03857.
[4] K. Adcox, Nucl. Phys. A 757 (2005) 184–283. Nucl-ex, arXiv:nucl-ex/0410003.
[5] J. Adams, Nucl. Phys. A 757 (2005) 102–183. Nucl-ex, arXiv:nucl-ex/0501009.
[6] A.M. Sirunyan, Eur. Phys. J. C 77 (4) (2017) 269. Nucl-ex, arXiv:1702.01462.
[7] R. Aaij, Phys. Lett. B 774 (2017) 159–178. Hep-ex, arXiv:1706.07122.
[8] S. Acharya, JHEP 07 (2023) 137. Nucl-ex, arXiv:2211.14153.
[9] M. Aaboud, Eur. Phys. J. C 78 (3) (2018) 171. ATLAS. nucl-ex, arXiv:1709.03089.
[10] J.P. Lansberg, A. Rakotozafindrabe, P. Artoisenet, D. Blaschke, J. Cugnon, D. Enterria, A.C. Kraan, F. Maltoni, D. Prorok, H. Satz, AIP Conf. Proc., 1038 (2008) 15–44. Hep-ph, arxiv:0807.3666.
[11] N. Brambilla, S. Eidelman, B.K. Heltsley, R. Vogt, G.T. Bodwin, E. Eichten, A.D. Frawley, A.B. Meyer, R.E. Mitchell, V. Papadimitriou, Eur. Phys. J. C 71 (2011) 1534. Hep-ph, arXiv:1010.5827.
[12] D. Kharzeev, E. Levin, M. Nardi, K. Tuchin, Nucl. Phys. A 826 (2009) 230–255. Hep-ph, arXiv:0809.2933.
[13] R.V. Gavai, S. Gupta, K. Sridhar, Nucl. Phys. A 498 (1989) 483C–488C.
[14] H. Satz, K. Sridhar, Phys. Rev. D 50 (1994) 3557–3559.
[15] R. Basu, K. Sridhar, Eur. Phys. J. C 34 (2004) 367–369. Hep-ph, arXiv:hep-ph/0301091.
[16] K. Zhou, N. Xu, Z. Xu, P. Zhuang, Phys. Rev. C 89 (5) (2014) 054911. PLXPAGE. nucl-th, arXiv:1401.5845.
[17] X. Du, R. Rapp, Nucl. Phys. A 943 (2015) 147–158. Hep-ph, arXiv:1504.00670.
[18] A. Andronic, P. Braun-Munzinger, M.K. Köhler, K. Redlich, J. Stachel, Phys. Lett. B 797 (2019) 134836. Nucl-th, arXiv:1901.09200.
[19] G.T. Bodwin, E. Braaten, G.P. Lepage, Phys. Rev. D 51 (1995) 1125. arXiv:hep-ph/9407339.
[20] F. Abe, Phys. Rev. Lett. 79 (1997) 572. Phys. Rev. Lett. 79 (1997) 578.
[21] D. Acosta, Phys. Rev. Lett. 88 (2002) 161802.
[22] R. Baier, R. Ruckl, Z. Phys. C 19 (1983) 251.
[23] T. Affolder, Phys. Rev. Lett. 85 (2000) 2886. arXiv:hep-ex/0004027. A. Abulencia, Phys. Rev. Lett. 99 (2007) 132001. arXiv:0704.0638. S. Chatrchyan, Phys. Lett. B 727 (2013) 381. arXiv:1307.6070. R. Aaij, Eur. Phys. J. C 73 (2013) 2631. arXiv:1307.6379.
[24] S. Chatrchyan, Phys. Rev. Lett. 110 (8) (2013) 081802. Hep-ex, arXiv:1209.2922.
[25] R. Aaij, JHEP 12 (2017) 110. Hep-ex, arXiv:1709.01301.
[26] K. Sridhar, Phys. Rev. Lett. 77 (1996) 4880–4883. Hep-ph, arXiv:hep-ph/9609285.
[27] K. Sridhar, Phys. Lett. B 674 (2009) 36–40. Hep-ph, arXiv:0812.0474.
[28] M. Cacciari, M. Kramer, Phys. Rev. Lett. 76 (1996) 4128. Hep-ph, arXiv:hep-ph/9601276]. J. Amundson, S. Fleming, I. Maksymyk, Phys. Rev. D 56 (1997) 5844. Hep-ph, arXiv:hep-ph/9601298. S. Gupta, K. Sridhar, Phys. Rev. D 54 (1996) 5545. Hep-ph, arXiv:hep-ph/9601349]. S. Gupta, K. Sridhar, Phys. Rev. D 55 (1997) 2650. Hep-ph, arXiv:hep-ph/9608433]]. M. Beneke, I. Z. Rothstein, Phys. Rev. D 54 (1996) 7082. Hep-ph, arXiv:hep-ph/9603400]]. W. K. Tang, M. Vanttinen, Phys. Rev. D 54 (1996) 4349. Hep-ph, arXiv:hep-ph/9603266]]. E. Braaten, Y. Q. Chen, Phys. Rev. Lett. 76 (1996) 730. Hep-ph, arXiv:hep-ph/9508373]]. K. M. Cheung, W. Y. Keung, T. C. Yuan, Phys. Rev. Lett. 76 (1996) 877. Hep-ph, arXiv:hep-ph/9509308]]. P. L. Cho, Phys. Lett. B 368 (1996) 171. Hep-ph, arXiv:hep-ph/9509355]]. K. M. Cheung, W. Y. Keung, T. C. Yuan, Phys. Rev. D 54 (1996) 929. Hep-ph, arXiv:hep-ph/9602423]]. P. Ko, J. Lee, H. S. Song, Phys. Rev. D 53 (1996) 1409. Hep-ph, arXiv:hep-ph/9510202]]. G. T. Bodwin, E. Braaten, T. C. Yuan, G. P. Lepage, Phys. Rev. D 46 (1992) 3703. Hep-ph, arXiv:hep-ph/9208254]]. K. Sridhar, A. D. Braaten, W. J. Stirling, Phys. Lett. B 438 (1998) 211. Hep-ph, arXiv:hep-ph/9806253]]. E. Braaten, B. A. Kniehl, J. Lee, Phys .Rev. D 62 (2000) 094005. Hep-ph, arXiv:hep-ph/9911436]].
[29] P. Mathews, P. Poulose, K. Sridhar, Phys. Lett. B 438 (1998) 336–340. Hep-ph, arXiv:hep-ph/9803424.
[30] S.S. Biswal, K. Sridhar, J. Phys. G 39 (2012) 015008. Hep-ph, arXiv:1007.5163.
[31] H. Han, Y.Q. Ma, C. Meng, H.S. Shao, Y.J. Zhang, K.T. Chao, Phys. Rev. D 94 (2016) 014028. Hep-ph, arXiv:1410.8537. Y. Feng, B. Gong, L.P. Wan, J.X. Wang, Chin. Phys. C 39 (2015) 123102. Hep-ph, arXiv:1503.08439. R. Li, J.X. Wang, Phys. Rev. D 99 (2019) 096010. Hep-ph, arXiv:1901.02141. B.A. Kniehl, V.A. Saleev, D.V. Vasin, Phys. Rev. D 94 (2006) 014024. Hep-ph, arXiv:hep-ph/0607254. K. Wang, Y.Q. Ma, K.T. Chao, Phys. Rev. D 85 (2012) 114003. Hep-ph, arXiv:1202.6012. B. Gong, J. X. Wang, H.F. Zhang, Phys. Rev. D 83 (2011) 114021. Hep-ph, arXiv:1009.3839. P. Artoisenet, J.M. Campbell, J.P. Lansberg, F. Maltoni, F. Tramontano, Phys. Rev. Lett. 101 (2008) 152001. Hep-ph, arXiv:0806.3282.
[32] S.S. Biswal, S.S. Mishra, K. Sridhar, Phys. Lett. B 832 (2022) 137221. Hep-ph, arXiv:2201.09393. Phys. Lett. B 834 (2022) 137490. Hep-ph, arXiv:2206.15252.
[33] S.S. Biswal, S.S. Mishra, K. Sridhar, JHEP 05 (2023) 120. Hep-ph, arXiv:2301.03158.
[34] S.S. Biswal, M. Mohanty, K. Sridhar, J. Subatomic Part. Cosmol. 3 (2025) 100026. Hep-ph, arxiv:2311.11233.
[35] S.S. Biswal, S.S. Mishra, M. Mohanty, K. Sridhar, Phys. Lett. B 859 (2024) 139108. Hep-ph, arXiv:2408.14133.
[36] M. Butenschoen, B.A. Kniehl, Mod. Phys. Lett. A 28 (2013) 1350027. Hep-ph, arXiv:1212.2037.
[37] S. Navas, Phys. Rev. D 110 (3) (2024) 030001.
[38] K. Kovarik, A. Kusina, T. Jezo, D.B. Clark, C. Keppel, F. Lyonnet, J.G. Morfin, F.I. Olness, J.F. Owens, I. Schienbein, Phys. Rev. D 93 (8) (2016) 085037. PLXPAGE. hep-ph, arXiv:1509.00792.
[39] L. Adamczyk, Phys. Lett. B 722 (2013) 55–62. Nucl-ex, arXiv:1208.2736.